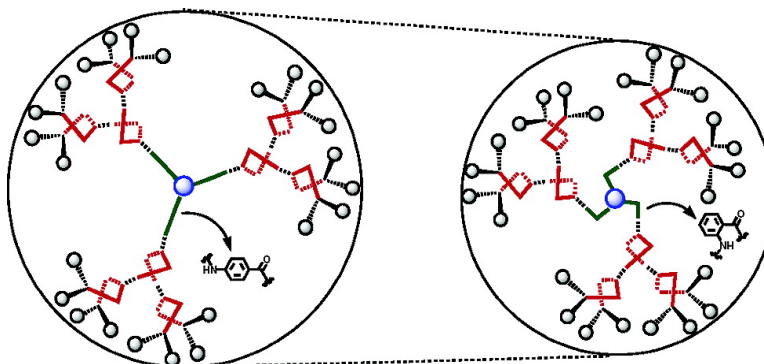


## The Effect of Global Compaction on the Local Secondary Structure of Folded Dendrimers

Baohua Huang, Matthew A. Prantil, Terry L. Gustafson, and Jon R. Parquette

*J. Am. Chem. Soc.*, **2003**, 125 (47), 14518-14530 • DOI: 10.1021/ja037895a • Publication Date (Web): 31 October 2003

Downloaded from <http://pubs.acs.org> on March 30, 2009



### More About This Article

Additional resources and features associated with this article are available within the HTML version:

- Supporting Information
- Links to the 5 articles that cite this article, as of the time of this article download
- Access to high resolution figures
- Links to articles and content related to this article
- Copyright permission to reproduce figures and/or text from this article

[View the Full Text HTML](#)

## The Effect of Global Compaction on the Local Secondary Structure of Folded Dendrimers

Baohua Huang, Matthew A. Prantil, Terry L. Gustafson, and Jon R. Parquette\*

*Contribution from the Department of Chemistry, The Ohio State University,  
Columbus, Ohio 43210*

Received August 12, 2003; E-mail: parquett@chemistry.ohio-state.edu

**Abstract:** The effect of nonlocal interactions on the local structural propensities of folded dendrimers was evaluated in this work by comparing, under identical conditions, the conformational properties of isomeric dendrimers differing in their global packing efficiency. Accordingly, a modular synthesis of two series of dendrimers up to the third generation was developed to provide efficient access to isomeric dendrimers displaying different levels of overall compaction. Dendrimer compaction levels were adjusted by connecting the folded dendrons to 1,3,5-benzenetricarbonyl chloride, as the central core, via either a 2- or a 4-aminobenzamide linkage to induce relatively "compacted" or "expanded" conformations, respectively. The hydrodynamic volumes of the dendrimers were measured by time-resolved fluorescence anisotropy (TRFA) measurements as a function of the dendrimer series, generation level, and solvent. Packing efficiencies (compaction levels) were estimated by the ratio ( $V_h/V_{vw}$ ) of the experimental hydrodynamic volume ( $V_h$ ) to the calculated van der Waals volume ( $V_{vw}$ ). The extent and stability of local helical bias was measured using circular dichroism and correlated with the packing efficiency ( $V_h/V_{vw}$ ). These studies suggested that compaction plays an extremely important role in determining the secondary structural preferences of the dendrimers; however, the nature of compaction was more important than the extent of compaction.

### Introduction

Many cellular functions such as catalysis, molecular recognition, and information storage are mediated by biomacromolecules that reversibly fold into compact, three-dimensional conformations.<sup>1</sup> The motivation for developing nonnatural oligomers capable of reversibly folding into unique structures is predicated on the notion that a capacity to control the long-range conformational equilibria of nonbiological materials will permit functions that lie outside the biological realm to be realized. Although many new folding oligomers, called "foldamers,"<sup>2</sup> have been reported that fold into compact secondary structures, functional biomolecules exhibit structures displaying much higher structural organization (tertiary and quaternary structure) that are likely to be necessary for function.<sup>1</sup> Recent progress toward the design of folding oligomers has produced an understanding of how primary structure can be programmed to afford stable secondary structural order through local non-covalent interactions. However, there is little information on how the long-range interaction of multiple elements of secondary structure affects the conformational properties of the molecule. An understanding of the nature of the local ↔ global conformational interplay would significantly assist the design of nonnatural molecules having tertiary structural order. Therefore,

the long-term goal of this work is directed at establishing control of the hierarchical folding process of a synthetic macromolecule by understanding how various elements of structural order cooperate to create a compact, three-dimensional structure.

Global compaction of a denatured protein into a condensed conformational state occurs early in the folding process of a protein into its native conformational state and is thought to be an important step in the folding reaction.<sup>3</sup> The cooperative interplay between large-scale organization and short-range local conformational propensities ultimately directs the folding process and determines the stability of the native state.<sup>4</sup> The effect of such long-range tertiary interactions on the formation and stability of short-range secondary structural order in natural protein macromolecules suggests that compacting a dendrimer structure into a condensed state will have a dramatic effect on the local conformational propensities of the dendrimer. However, the degree of cooperativity between the collapse of a protein into a compact shape and the development of secondary structure is not well understood. For example, early lattice model studies suggested that the nonlocal interactions that drive protein collapse are strongly coupled to the formation of secondary structure and that compaction alone is sufficient to create secondary structure in proteins.<sup>5,6</sup> Several subsequent theoretical<sup>7</sup> and experimental<sup>8</sup> studies concluded that the degree of local ↔

(1) Creighton, T. E. *Proteins. Structure and Molecular Principles*; W. H. Freeman and Company: New York, 1993.

(2) (a) Hill, D. J.; Mio, M. J.; Prince, R. B.; Hughes, T. S.; Moore, J. S. *Chem. Rev.* **2001**, *101*, 3893. (b) Cheng, R. P.; Gellman, S. H.; DeGrado, W. F. *Chem. Rev.* **2001**, *101*, 3219. (c) Gellman, S. H. *Acc. Chem. Res.* **1998**, *31*, 173.

(3) (a) Chahine, J.; Nymeyer, H.; Leite, V. B. P.; Socci, N. D.; Onuchic, J. N. *Phys. Rev. Lett.* **2002**, *88*, 168101-1. (b) Uversky, V. N.; Fink, A. L. *FEBS Lett.* **2002**, *515*, 79.

(4) Niggemann, M.; Steipe, B. *J. Mol. Biol.* **2000**, *296*, 181 and references therein.

global cooperativity was low when the collapse transition was driven only by nonspecific, long-range interactions. Nevertheless, the importance of both short- and long-range interactions in stabilizing the folded state of a protein can be inferred from the observation that isolated  $\alpha$ -helices are rarely stable in water<sup>9</sup> and that protein fragments often exhibit different conformational properties in the absence of the tertiary structure of the intact protein.<sup>10</sup> There also is a good correlation between the relative decrease in hydrodynamic volume and the increase in secondary structure content among proteins in the literature.<sup>3b,11</sup> Similarly, the hydrophobic interiors of proteins, in their native state, maintain an extremely high packing density of side chains similar to the packing found in organic solids.<sup>12</sup> This efficient filling of internal space in a protein appears to be an important determinant of protein stability<sup>13</sup> and is thought to be a crucial factor responsible for the remarkable thermal stability of thermophilic proteins.<sup>14,15</sup> Consequently, the organization of elements of protein secondary structure on a template has become an effective tool for inducing and stabilizing secondary and tertiary structures of a variety of folding motifs.<sup>16</sup>

The highly branched and regularly repeating connectivity of dendritic macromolecules creates a three-dimensional structure that adopts an increasingly compact, globular shape at higher generations,<sup>17,18</sup> potentially mimicking the morphology of globular proteins.<sup>19</sup> Consequently, dendrimers would seem to present an opportunity to approach the design and synthesis of

macromolecules in which multiple elements of secondary structure can interact intramolecularly. Based on the studies described above, the induction of secondary structural order in dendrimeric macromolecules should be enhanced by the compact structure of higher generations. However, in many dendrimer systems, significant backfolding of the termini occurs, indicating a certain lack of local conformational order in the dendrimer structure.<sup>20</sup> This internal flexibility appears to be responsible for the difficulties experienced in efforts to develop three-dimensional organization in these systems,<sup>21,22</sup> and recent efforts in our laboratory to compact polyaryl ether dendrimers in aqueous media indicated that compaction alone was not a sufficient criterion to induce secondary structure in flexible dendrimers.<sup>24</sup>

## Design Considerations

Recently, we described a series of dendrons whose local conformational properties were restricted through the intervention of intramolecular hydrogen-bonding and electrostatic interactions present in the AB<sub>2</sub> building block (Figure 1, bottom).<sup>25</sup> These dendrons adopt a specific, chiral helical secondary structure that occurs throughout the internal and peripheral regions and depends critically on the development of intramolecular packing interactions at higher dendron generation (Figure 1, top). These nonbonded packing interactions couple the motions and conformational preferences of each pair of terminal groups, or helical fold, causing the highly dynamic equilibrium interconverting the M and P helical conformations shown below to shift toward a single helical sense.<sup>26</sup>

- (5) (a) Chan, H. S.; Dill, K. A. *Macromolecules* **1989**, *22*, 4559. (b) Chan, H. S.; Dill, K. A. *Proc. Natl. Acad. Sci. U.S.A.* **1990**, *87*, 6388. (c) Dill, K. A.; Bromberg, S.; Yue, K.; Fiebig, K. M.; Yee, D. P.; Thomas, P. D.; Chan, H. S. *Protein Sci.* **1995**, *4*, 561. (d) Thomas, P. D.; Dill, K. A. *Protein Sci.* **1993**, *2*, 2050. (e) Yue, K.; Dill, K. A. *Proc. Natl. Acad. Sci. U.S.A.* **1995**, *92*, 146. (f) Go, N.; Taketomi, H. *Proc. Natl. Acad. Sci. U.S.A.* **1978**, *75*, 559.
- (6) Fersht, A. R.; Shakhnovich, E. I. *Curr. Biol.* **1998**, *8*, R478.
- (7) (a) Chou, J. J.; Shakhnovich, E. I. *J. Phys. Chem. B* **1999**, *103*, 2535. (b) Go, N.; Taketomi, H. *Proc. Natl. Acad. Sci. U.S.A.* **1978**, *75*, 559. (c) Gregoret, L. M.; Cohen, F. E. *J. Mol. Biol.* **1991**, *219*, 109. (d) Kolinski, A.; Madziar, P. *Biopolymers* **1997**, *42*, 537. (e) Kolinski, A.; Skolnick, J. *Proteins: Struct., Funct., Genet.* **1994**, *18*, 338.
- (8) (a) Gast, K.; Chaffotte, A. F.; Zirwer, D.; Guillou, Y.; Mueller-Frohne, M.; Cadioux, C.; Hodges, M.; Damaschun, G.; Goldberg, M. E. *Protein Sci.* **1997**, *6*, 2578. (b) Mizuguchi, M.; Masaki, K.; Demura, M.; Nitta, K. *J. Mol. Biol.* **2000**, *298*, 985. (c) Yee, D. P.; Chan, H. S.; Havel, T. F.; Dill, K. A. *J. Mol. Biol.* **1994**, *241*, 557.
- (9) (a) Chakrabarty, A.; Baldwin, R. L. *Adv. Protein Chem.* **1995**, *46*, 14. (b) Chakrabarty, A.; Kortemme, T.; Baldwin, R. L. *Protein Sci.* **1994**, *3*, 843. (c) Chakrabarty, A.; Schellman, J. A.; Baldwin, R. L. *Nature* **1991**, *351*, 586. (d) Rohl, C. A.; Chakrabarty, A.; Baldwin, R. L. *Protein Sci.* **1996**, *5*, 2623.
- (10) Hyde, C. C.; Ahmed, S. A.; Padlan, E. A.; Miles, E. W.; Davies, D. R. *J. Biol. Chem.* **1988**, *263*, 17857.
- (11) (a) Gualfetti, P. J.; Bilsel, O.; Matthews, C. R. *Protein Sci.* **1999**, *8*, 1623. (b) Gualfetti, P. J.; Iwakura, M.; Lee, J. C.; Kihara, H.; Bilsel, O.; Zitzewitz, J. A.; Matthews, C. R. *Biochemistry* **1999**, *38*, 13367.
- (12) (a) Fleming, P. J.; Richards, F. M. *J. Mol. Biol.* **2000**, *299*, 487. (b) Gualfetti, P. J.; Iwakura, M.; Lee, J. C.; Kihara, H.; Bilsel, O.; Zitzewitz, J. A.; Matthews, C. R. *Biochemistry* **1999**, *38*, 13367. (c) Liang, J.; Dill, K. A. *Biophys. J.* **2001**, *81*, 751.
- (13) (a) Gregoret, L. M.; Cohen, F. E. *J. Mol. Biol.* **1991**, *219*, 109. (b) Richards, F. M. *Cell. Mol. Life Sci.* **1997**, *53*, 790. (c) Levitt, M.; Gerstein, M.; Huang, E.; Subbiah, S.; Tsai, J. *Annu. Rev. Biochem.* **1997**, *66*, 549. (d) Jaenicke, R.; Bohm, G. *Curr. Opin. Struct. Biol.* **1998**, *8*, 738. (e) Jaenicke, R. *J. Biotechnol.* **2000**, *79*, 193. (f) Kussell, E.; Shimada, J.; Shakhnovich, E. I. *J. Mol. Biol.* **2001**, *311*, 183.
- (14) (a) Russell, R. J. M.; Taylor, G. L. *Curr. Opin. Biotechnol.* **1995**, *6*, 370. (b) Jaenicke, R. *Proc. Natl. Acad. Sci. U.S.A.* **2000**, *97*, 2962. (c) Kumar, S.; Nussinov, R. *Cell. Mol. Life Sci.* **2001**, *58*, 1216. (d) Perl, D.; Schmid, F. X. *ChemBioChem* **2002**, *3*, 39.
- (15) (a) Mutter, M.; Tuchscherer, G. *Cell. Mol. Life Sci.* **1997**, *53*, 851. (b) Ramachandran, S.; Udgaonkar, J. B. *Biochemistry* **1996**, *35*, 8776.
- (16) For some reviews of templated assembled synthetic proteins (TASP), see: (a) Mutter, M.; Dumy, P.; Garrouste, P.; Lehmann, C.; Mathieu, M.; Peggion, C.; Peluso, S.; Razzaname, A.; Tuchscherer, G. *Angew. Chem., Int. Ed. Engl.* **1996**, *35*, 1482. (b) Tuchscherer, G.; Mutter, M. *Pure Appl. Chem.* **1996**, *68*, 2153. (c) Tuchscherer, G.; Grell, D.; Mathieu, M.; Mutter, M. *J. Pept. Res.* **1999**, *54*, 185.
- (17) For a review, see: Bosman, A. W.; Janssen, H. M.; Meijer, E. W. *Chem. Rev.* **1999**, *99*, 1665.
- (18) (a) Mansfield, M. L.; Klushin, L. I. *J. Phys. Chem.* **1992**, *96*, 3994. (b) Mourey, T. H.; Turner, S. R.; Rubinstein, M.; Frechet, J. M. J.; Hawker, C. J.; Wooley, K. L. *Macromolecules* **1992**, *25*, 2401. (c) Cai, C.; Chen, Z. Y. *Macromolecules* **1998**, *31*, 6393. (d) Scherrenberg, R.; Coussens, B.; van Vliet, P.; Edouard, G.; Brackman, J.; de Brabander, E.; Mortensen, K. *Macromolecules* **1998**, *31*, 456. (e) Ganazzoli, F.; La Ferla, R.; Terragni, G. *Macromolecules* **2000**, *33*, 6611. (f) Jeong, M.; Mackay, M. E.; Vestberg, R.; Hawker, C. J. *Macromolecules* **2001**, *34*, 4927. (g) Tande, B. M.; Wagner, N. J.; Mackay, M. E.; Hawker, C. J.; Jeong, M. *Macromolecules* **2001**, *34*, 8580.
- (19) Newkome, G. R.; Moorefield, C. N.; Vogtle, F. F. *Dendritic Molecules: Concepts, Syntheses, Perspectives*; VCH: Weinheim, New York, 1996.
- (20) (a) Epperson, J. D.; Ming, L.-J.; Baker, G. R.; Newkome, G. R. *J. Am. Chem. Soc.* **2001**, *123*, 8583. (b) Epperson, J. D.; Ming, L.-J.; Woosley, B. D.; Baker, G. R.; Newkome, G. R. *Inorg. Chem.* **1999**, *38*, 4498. (c) Wooley, K. L.; Klug, C. A.; Tasaki, K.; Schaefer, J. *J. Am. Chem. Soc.* **1997**, *119*, 53.
- (21) For some reviews of the conformational properties of chiral dendrimers, see: (a) Ramagnoli, B.; Hayes, W. *J. Mater. Chem.* **2002**, *12*, 767. (b) Seebach, D.; Rheiner, P. B.; Greiveldinger, G.; Butz, T.; Sellner, H. *Top. Curr. Chem.* **1998**, *197*, 125. (c) Thomas, C. W.; Tor, Y. *Chirality* **1998**, *10*, 53. (d) Peerlings, H. W. I.; Meijer, E. W. *Chem.-Eur. J.* **1997**, *3*, 1563.
- (22) Laufferweiler, M. J.; Rohde, J. M.; Chaumette, J.-L.; Sarazin, D.; Parquette, J. R. *J. Org. Chem.* **2001**, *66*, 6440.
- (23) For notable examples of the effect of dendrimer constitution on structure and function, see: (a) Chasse, T. L.; Sachdeva, R.; Li, Q.; Li, Z.; Petrie, R. J.; Gorman, C. B. *J. Am. Chem. Soc.* **2003**, *125*, 8250. (b) Harth, E. M.; Hecht, S.; Helms, B.; Malmstrom, E. E.; Frechet, J. M. J.; Hawker, C. J. *J. Am. Chem. Soc.* **2002**, *124*, 3926. (c) Jeong, M.; Mackay, M. E.; Vestberg, R.; Hawker, C. J. *Macromolecules* **2001**, *34*, 4927. (d) Peerlings, H. W. I.; Trimbach, D. C.; Meijer, E. W. *Chem. Commun.* **1998**, 497. (e) Peng, Z.; Pan, Y.; Xu, B.; Zhang, J. *J. Am. Chem. Soc.* **2000**, *122*, 6619. (f) Rosini, C.; Superchi, S.; Peerlings, H. W. I.; Meijer, E. W. *Eur. J. Org. Chem.* **2000**, 61.
- (24) Weintraub, J. G.; Broxer, S.; Paul, N. M.; Parquette, J. R. *Tetrahedron* **2001**, *57*, 9393.
- (25) (a) Huang, B.; Parquette, J. R. *Org. Lett.* **2000**, *2*, 239. (b) Recker, J.; Tomcik, D. J.; Parquette, J. R. *J. Am. Chem. Soc.* **2000**, *122*, 10298. (c) Gandhi, P.; Huang, B.; Gallucci, J. C.; Parquette, J. R. *Org. Lett.* **2001**, *3*, 3129. (d) Huang, B.; Parquette, J. R. *J. Am. Chem. Soc.* **2001**, *123*, 2689.
- (26) Although the barrier could not be measured for these dendrons, we have recently measured a barrier of 12.3 kcal/mol in a related pyridine-2,6-diamide system using NMR line-shape analysis. This barrier most likely represents an upper limit for the dendrons and dendrimers described in this manuscript. Preston, A. J.; Fraenkel, G.; Chow, A.; Gallucci, J. C.; Parquette, J. R. *J. Org. Chem.* **2003**, *68*, 22.

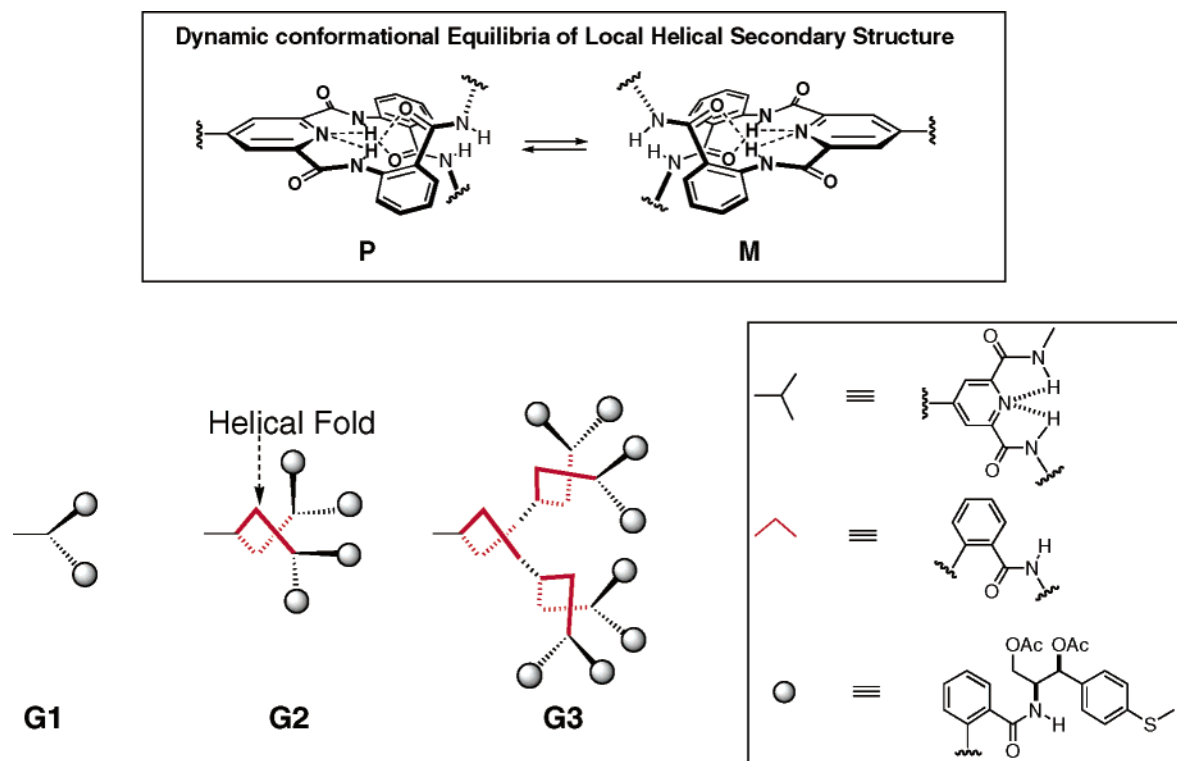


**Figure 1.** Structure and conformational equilibria of helically folded dendrons.

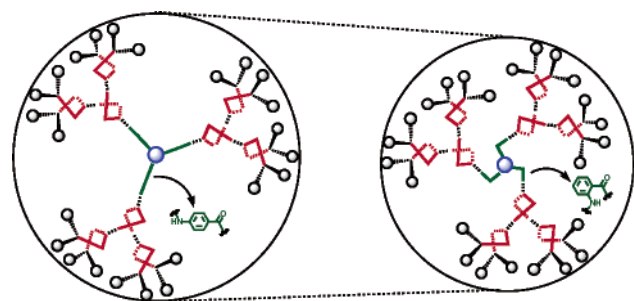


**Figure 2.** Notional depiction of structural compaction of a folded dendrimer.

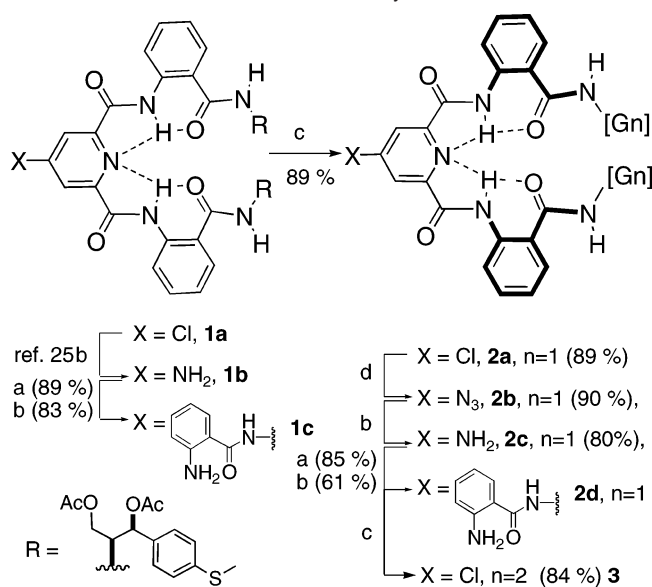
Correlating this local helical conformational equilibria with the nonlocal interactions experienced between adjacent dendrons requires a capability to compare the conformational properties of isomeric dendrimers differing only in their global packing efficiency.<sup>23</sup> However, previous studies addressing the effect of structure on the hydrodynamic properties of dendrimers have reported that relatively minor structural modifications, such as those observed in the *cis/trans* photoisomerization of azobenzene dendron/core linkages, induce comparatively small volume changes in flexible dendrimers.<sup>27</sup> Fortuitously, relatively minor modifications of the dendron/core linkage in the structure of these folded dendrimers afforded large variations in hydrodynamic volumes, thereby allowing the effect of compaction on local secondary structure to be investigated in isomeric systems having minimal constitutional differences (Figure 2). Accordingly, attaching the dendrons to the central core via either 4-aminobenzamide (*para*) or 2-aminobenzamide (*ortho*) linkage produced structures with significantly different hydrodynamic

volumes. Specifically, the *ortho* linkage provided dendrimers with a more compact structure (smaller hydrodynamic volume) than did the isomeric *para* linkage.

### Dendron Synthesis: First-Generation Strategy

We previously reported a synthetic strategy toward dendrons having a 2-aminobenzamide linkage at each generational shell that employed 4-chloropyridine-2,6-dicarbonyl chloride as the branching monomer.<sup>25d</sup> Convergent generational growth was accomplished using amide bond-forming reactions, and focal point activation occurred by  $\text{NaN}_3$  displacement of the focal chloro group followed by hydrogenation (Scheme 1). Acylation of the focal amino group of a dendron followed by hydrogenation over Pd/C installed a 2-aminobenzamide moiety that became the connecting unit between generational levels upon reaction with 4-chloropyridine-2,6-dicarbonyl chloride. Although this strategy provided dendrons up to the third generation, there were three issues that needed to be addressed to efficiently construct larger dendrimers from these dendron precursors. First, attaching the 2-aminobenzamide connector at each generational level by this process was a strictly linear strategy and required five transformations for each generational growth step. Second, the focal amino group at each generation was severely deactivated by the electron-deficient pyridine ring, causing the reaction with 2-nitrobenzoyl chloride to be slow and capricious, particularly on a large scale. Finally, hydrogenation of the nitro group proceeded much more slowly (2–3 d) than was expected for a nitro function presumably due to poisoning of the catalyst by the dendron structure.<sup>28</sup> Therefore, a more convergent strategy that circumvented these limitations was developed to improve the efficiency of the dendrimer synthesis.

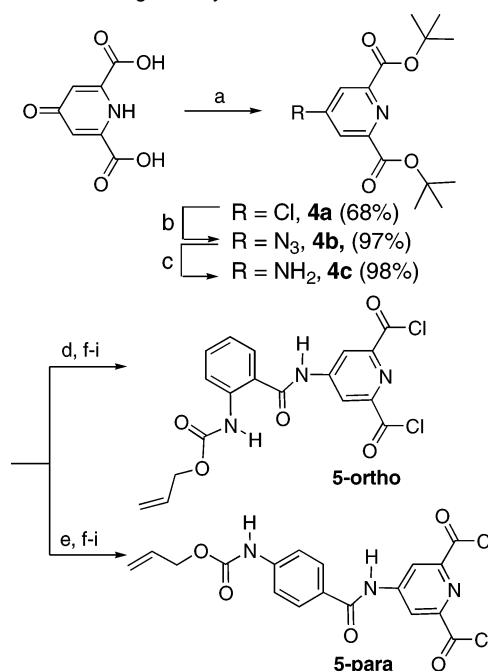
(27) (a) Junge, D. M.; McGrath, D. V. *J. Am. Chem. Soc.* **1999**, *121*, 4912. (b) Li, S.; McGrath, D. V. *J. Am. Chem. Soc.* **2000**, *122*, 6795. (c) Liao, L.-X.; Junge, D. M.; McGrath, D. V. *Macromolecules* **2002**, *35*, 319.

**Scheme 1.** First-Generation Dendron Synthesis<sup>a</sup>

<sup>a</sup> (a) 2-NO<sub>2</sub>C<sub>6</sub>H<sub>4</sub>COCl, pyr., (b) H<sub>2</sub>, Pd-C, EtOAc-CH<sub>3</sub>OH, (c) 4-chloropyridine-2,6-dicarboxyl chloride, pyr., (d) NaN<sub>3</sub>, DMF, 50 °C.

### Second-Generation Strategy: Synthesis of Functionalized Branching Monomers

We envisioned that employing a branching moiety functionalized at the 4-position with a suitably protected 2- or 4-aminobenzamide connector would address all three limitations of the initial synthetic strategy. Directly incorporating the turn unit in the branching unit would decrease each generational growth step by three transformations, and the problematic amine acylation and subsequent nitro reduction steps would only need to be addressed once in a relatively simple molecule rather than at every generational step. This strategy would also provide the flexibility to construct dendrons with a 4-aminobenzamide linkage at the focal point by employing an appropriately functionalized branching moiety just prior to attachment to a dendrimeric central core. Accordingly, exposure of chelidamic acid to phosphorus oxychloride at 128 °C followed by reaction of the crude acid chloride with *tert*-butyl alcohol provides *tert*-butyl-4-chloropyridine-2,6-dicarboxylate **4a** in 68% yield (Scheme 2). The use of *tert*-butyl esters was necessary to avoid intramolecular cleavage of the benzamido linkage by the carbamate linkage that occurred when the analogous propyl dicarboxylate of **5-ortho** was exposed to basic hydrolysis conditions. Extension of the focal function was achieved by sodium azide displacement followed by hydrogenation affording amine **4c**. Reaction of **4c** with either 2-nitro- or 4-nitrobenzoyl chloride followed by hydrogenation, acylation with allyl chloroformate, and deprotection of the *tert*-butyl esters with CF<sub>3</sub>-CO<sub>2</sub>H/CH<sub>2</sub>Cl<sub>2</sub> (1:1) afforded, after conversion to the corresponding acid chlorides with oxalyl chloride, branching units **5-ortho** and **5-para**.

**Scheme 2.** Branching Unit Synthesis<sup>a</sup>

<sup>a</sup> (a) (i) POCl<sub>3</sub>, 128 °C, 12 h, (ii) *t*-C<sub>4</sub>H<sub>9</sub>OH, DMAP (cat.), CH<sub>2</sub>Cl<sub>2</sub>/pyr., 12 h, (b) NaN<sub>3</sub>, DMF, 50 °C, (c) H<sub>2</sub>, Pd-C, EtOAc-CH<sub>3</sub>OH, (d) 2-nitrobenzoyl chloride, DMAP (cat.), CH<sub>2</sub>Cl<sub>2</sub>/pyr., 4 h (93%), (e) 4-nitrobenzoyl chloride, DMAP (cat.), CH<sub>2</sub>Cl<sub>2</sub>/pyr., 6 h (87%), (f) H<sub>2</sub>, Pd-C, EtOAc-CH<sub>3</sub>OH (95% for **5-ortho**, 85% for **5-para**), (g) allyl chloroformate, DMAP (cat.), CH<sub>2</sub>Cl<sub>2</sub>/pyr., (82% for **5-ortho**, 91% for **5-para**), (h) CF<sub>3</sub>CO<sub>2</sub>H/CH<sub>2</sub>Cl<sub>2</sub> (1:1), 2.5 h, 92% (for **5-ortho** and **5-para**), (i) **5-ortho** or **5-para**, (COCl)<sub>2</sub>, CH<sub>2</sub>Cl<sub>2</sub>, DMF (cat.).

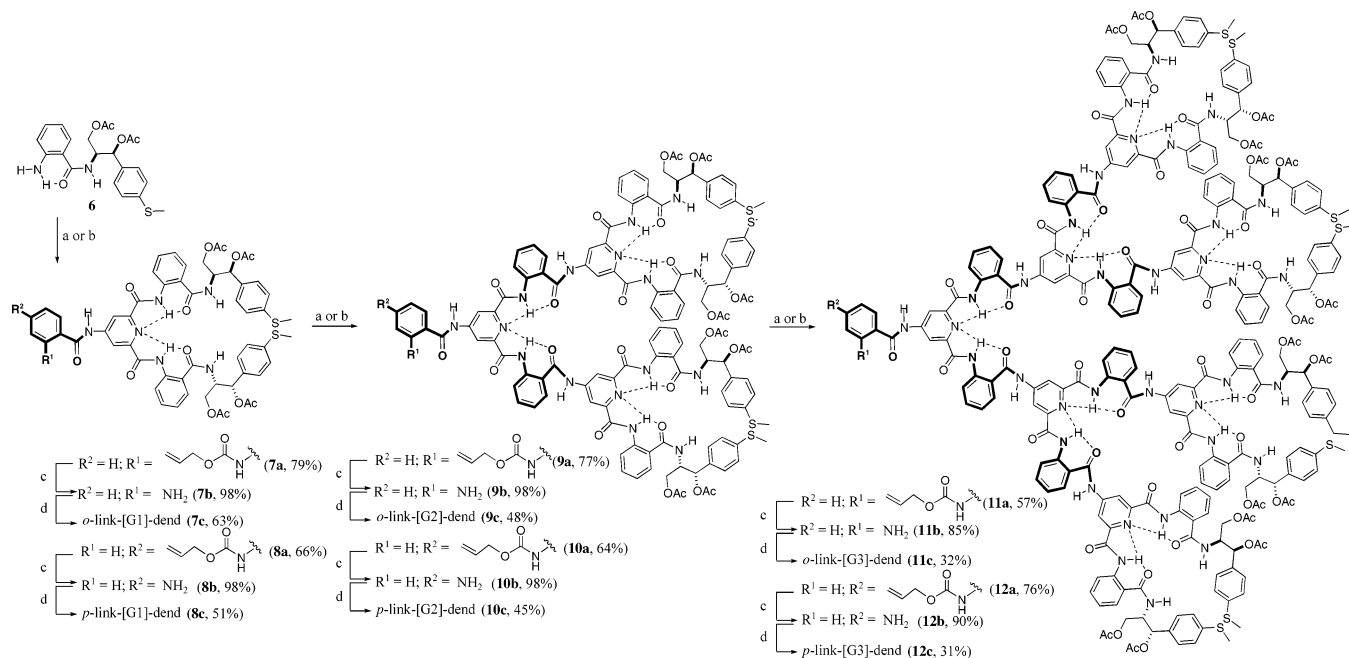
### Dendron Synthesis

Construction of the focal point derivatized dendrons proceeded in a convergent manner by treating **5-ortho** with 2 equiv of amine **6**,<sup>25b</sup> thereby providing first-generation dendron **7a** in 79% yield (Scheme 3). Deprotection of the *N*-allyloxycarbonyl group of the anthranilamide connector using a catalyst prepared from 2.5 mol % Pd<sub>2</sub>(dba)<sub>3</sub>-CHCl<sub>3</sub>/25 mol % PPh<sub>3</sub> and tributylammonium formate as a nucleophile provided the free amine (**7b**, 46%) along with equal amounts of the corresponding *N*-allyl derivative (46%), which was difficult to separate chromatographically. This side product was formed by nucleophilic attack on the palladium  $\pi$ -allyl complex by the amino group of the product, generated by the deprotection, and occurred in competition with capture by ammonium formate. Employing dimedone as a more nucleophilic acceptor<sup>29</sup> provided the free amine in 90% yield; however, this material contained approximately 10% of the *N*-allyl compound as an inseparable impurity. When *N,N'*-dimethylbarbituric acid was utilized as allyl acceptor,<sup>30</sup> deprotection reproducibly provided 98% yield of amine **7b** after 30 min at ambient temperature without contamination by the *N*-allyl byproduct. Subsequent reaction of amine **7b** with **5-ortho** followed by deprotection with the Pd(0) catalyst afforded second-generation dendron **9b** in good yield and high purity. Repetition of the generational growth and deprotection steps afforded third-generation dendron **11b**.

(28) We conclude that the decreased hydrogenation rate is due to catalyst poisoning rather than steric encumbrance for two reasons. (1) Hydrogenation is relatively slow even for first-generation dendron **1b**. (2) These dendrons are known to efficiently coordinate to transition metals, see: Rauckhorst, M. R.; Wilson, P. J.; Hatcher, S. A.; Hadad, C. M.; Parquette, J. R. *Tetrahedron* **2003**, *59*, 3917.

(29) Kunz, H.; Unverzagt, C. *Angew. Chem.* **1984**, *96*, 426.

(30) Kunz, H.; Maerz, J. *Angew. Chem.* **1988**, *100*, 1424.

**Scheme 3.** Second-Generation Dendrimer Synthesis<sup>a</sup>

## Dendrimer Synthesis

Dendrimers were prepared by linking the dendrons to 1,3,5-benzene tricarboxyl chloride through either a 2-aminobenzamide or a 4-aminobenzamide connecting unit to create isomeric dendrimers differing only in their hydrodynamic volumes. The appropriate connector was introduced by reacting with either **5-ortho** or **5-para** in the generational growth step just preceding reaction with the core to form a particular dendrimer generation. For example, dendrimers containing a 4-aminobenzamide linkage to the central core were prepared by reacting amines **6**, **7b**, or **9b** with **5-para**, affording dendrons having a 4-aminobenzamide group (para-linked) at the focal point (**8b**, **10b**, and **12b**) following deprotection (Scheme 3). These para-linked dendrons were subsequently reacted with 1,3,5-benzenetricarbonyl chloride, giving the first (*p*-link[G1]-dend, **8c**-), second (*p*-link[G2]-dend, **10c**-), or third (*p*-link[G3]-dend, **12c**-) generation dendrimers (Figure 4). Similarly, to prepare the ortho-linked dendrimers, amines **6**, **7b**, or **9b** were treated with **5-ortho**, affording, after deprotection, the corresponding ortho-linked dendrons **7b**, **9b**, and **11b**, respectively. Reaction with 1,3,5-benzenetricarbonyl chloride in pyridine–CH<sub>2</sub>Cl<sub>2</sub> afforded the first (*o*-link[G1]-dend, **7c**-), second (*o*-link[G2]-dend, **9c**-) or third (*o*-link[G3]-dend, **11c**-) generation dendrimers (Figure 3). All dendrons and dendrimers displayed <sup>1</sup>H and <sup>13</sup>C NMR spectra, along with mass spectra and elemental analyses, consistent with the expected structures.

## Steady-State Absorption and Emission Properties

Ultraviolet–visible absorption (UV–vis) and fluorescence spectra of dendrons **1a–2a**, **3**, and dendrimers **7c–12c** are shown in Figure 5. The transition in the UV–vis spectrum that occurs at 316 nm corresponds to a  $\pi \rightarrow \pi^*$  excitation of the 2-acylamino benzamide chromophores present throughout the dendrimer structures.<sup>25</sup> 2-Aminobenzamide chromophores have

been used extensively as fluorescent probes because of the high quantum yield of fluorescence, thereby enabling the dendrimers to be studied by fluorescence depolarization.<sup>31</sup> Accordingly, upon excitation at 300 nm, all of the dendrons and dendrimers exhibited a broad emission band in the range of 350–590 nm with apparent maxima at approximately 425 and 460 nm. Significantly lower fluorescence quantum yields were observed for the dendrons/dendrimers relative to simple 2-acylamino benzamides. The lower quantum yields may be a consequence of the deviation of the amides in the dendritic structures from periplanarity inducing nonradiative processes to contribute to the deactivation of the excited state.<sup>31b</sup> At higher generations, the intensity of the emission band at 425 nm increased relative to that of the 460 nm band. This behavior may have been due to a variation in the absorption characteristics of the dendrimers that would result in different chromophores being excited at 300 nm as a function of dendrimer structure and generation. To examine this possibility, the relative emission intensity at 425 and 460 nm was monitored as the excitation wavelength was scanned from 250 to 400 nm for dendron **3** and dendrimer **7c**. However, the relative intensity of the two emission bands did not vary over that excitation range, thus ruling out this possibility. The fluorescence spectra similarly did not depend on concentration (within the range of 10<sup>−6</sup>–10<sup>−8</sup> M) or solvent quality (THF, CH<sub>2</sub>Cl<sub>2</sub>, 10–50% EtOH/CH<sub>2</sub>Cl<sub>2</sub>, MeCN, 10–50% MeCN/EtOH), indicating that intermolecular aggregation or solvent-induced structural collapse was not responsible (see Table 1 in Supporting Information and Figure 6 for the effect of solvent on compaction). Lifetime data were then collected for **3** and **7c** at 10–20 nm increments across the fluorescence

(31) (a) Ferro, V.; Weiler, L.; Withers, S. G. *Carbohydr. Res.* **1998**, *306*, 531. (b) Ito, A. S.; Turchiello, R. d. F.; Hirata, I. Y.; Cezari, M. H. S.; Meldal, M.; Juliano, L. *Biospectroscopy* **1998**, *4*, 395. (c) Turchiello, R. F.; Lamy-Freund, M. T.; Hirata, I. Y.; Juliano, L.; Ito, A. S. *Biophys. Chem.* **1998**, *73*, 217.

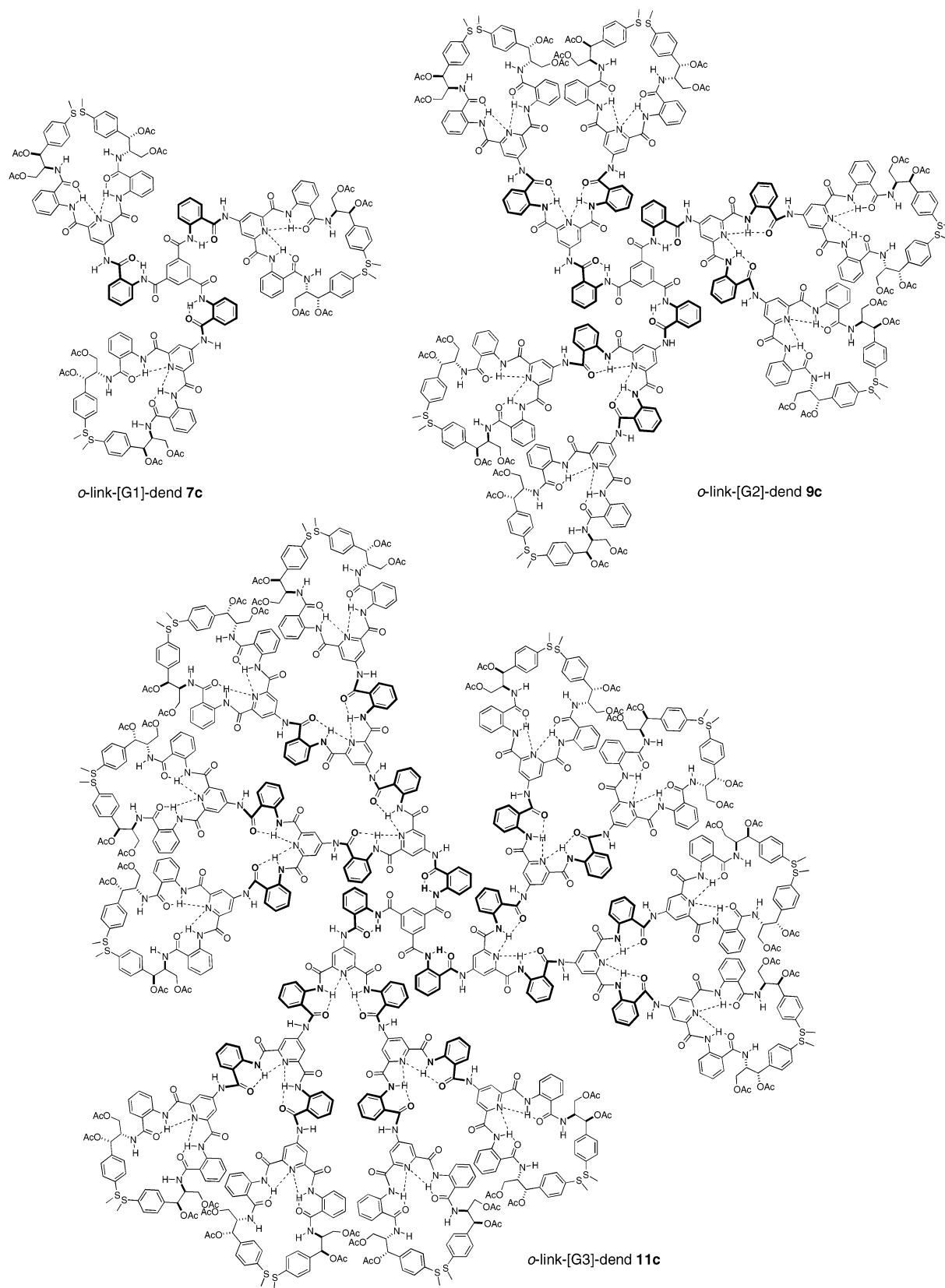


**Figure 3.** Structures of “compact” dendrimers constructed with an *ortho*-aminobenzamide linkage.

region (380–500 nm), and all of the spectra yielded four distinct lifetimes upon fitting the data with discrete exponentials (Figure 1, Supporting Information).<sup>32</sup> These lifetime values, both relative

population and lifetime, only varied slightly across the spectral region, indicating that the two apparent maxima in the fluorescence were not a consequence of unique intramolecular excited-

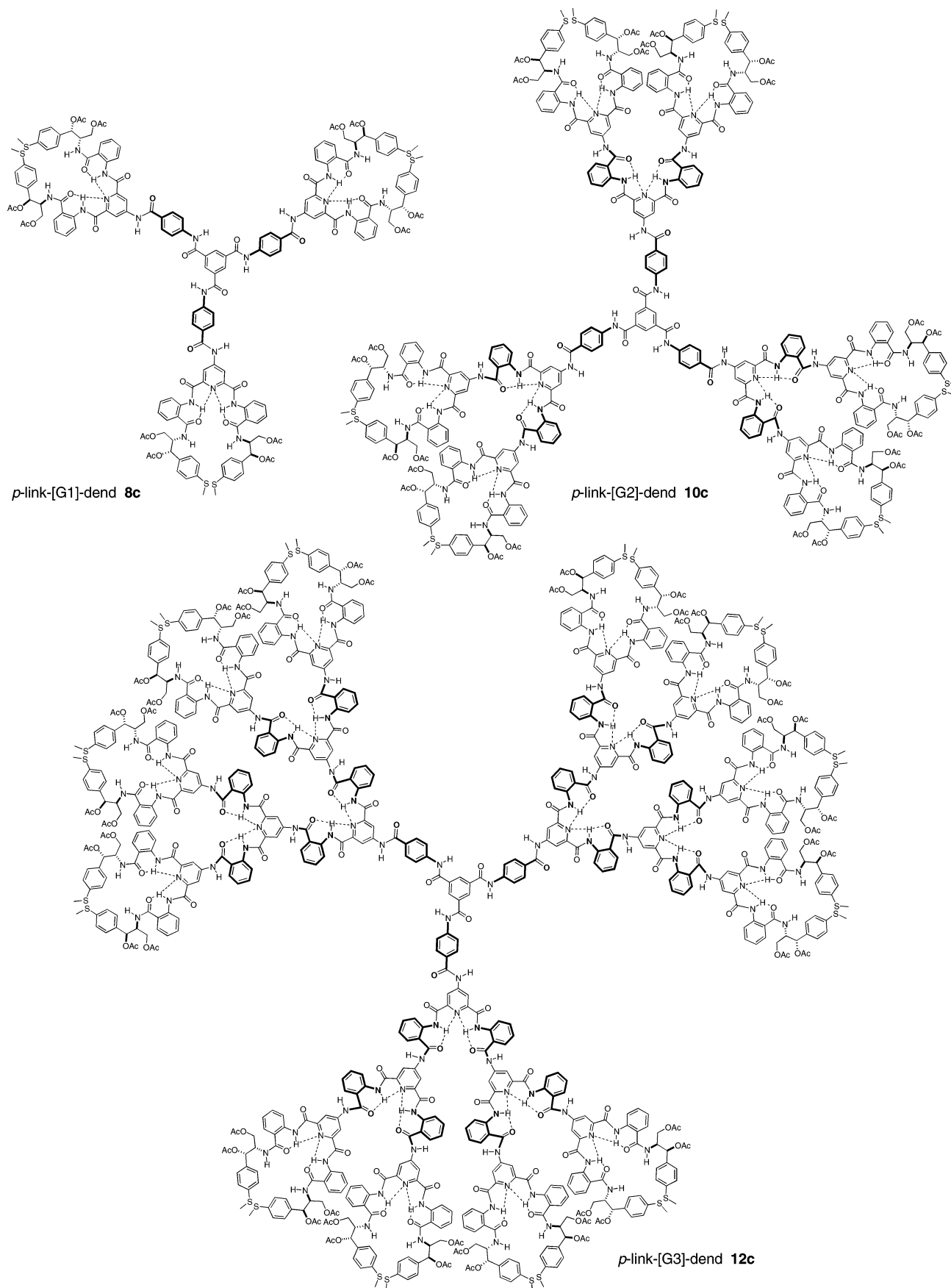


**Figure 4.** Structure of “expanded” dendrimers constructed from a *para*-aminobenzamide linkage.

state dimers (excimers or exciplexes) or of the localized emission of multiple, different chromophores.<sup>33</sup> Rather, the appearance

and variation in the spectra likely reflect conformational differences and the emission of spatially delocalized excitons.<sup>34</sup>



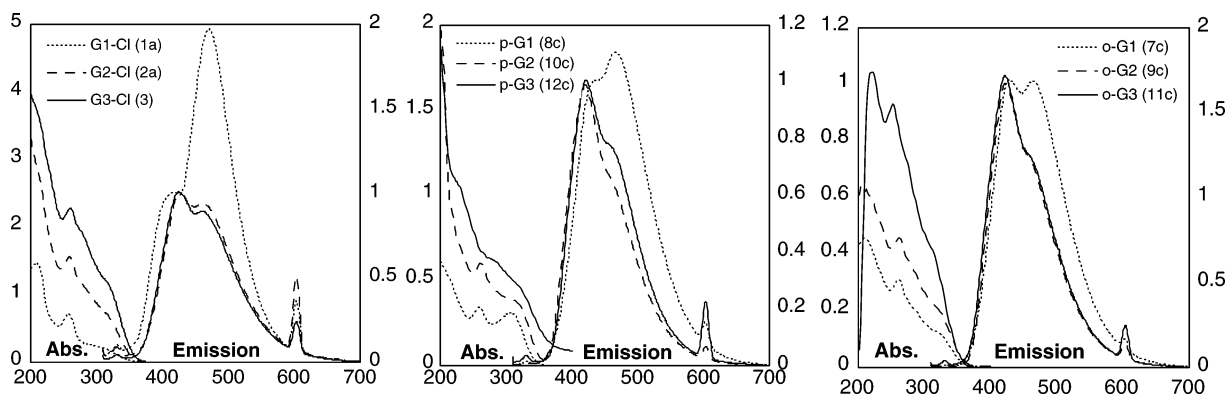


**Figure 5.** Absorption and emission spectra of dendrons **1a–2a, 3**, and dendrimers **7c–12c**. Spectra normalized for comparison. Quantum yields:<sup>35</sup> **1a** (0.004), **2a** (0.002), **3** (0.004), **8c** (0.011), **10c** (0.009), **12c** (0.011), **7c** (0.007), **9c** (0.011), **11c** (0.011).

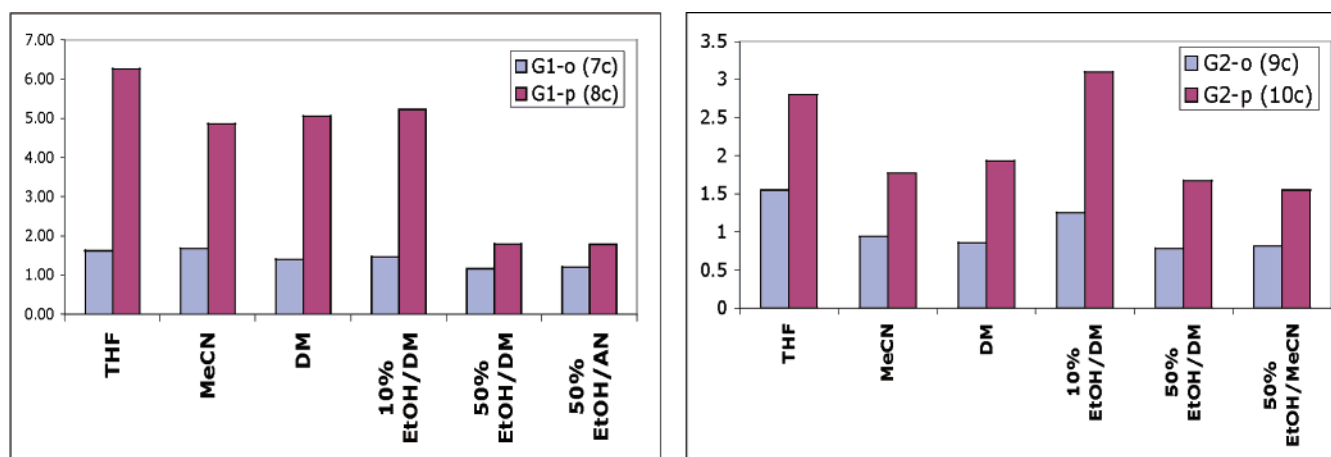


**Figure 6.** Packing efficiencies ( $V_h/V_{vw}$ ) of dendrimers **7c–10c** as a function of solvent.

### Time-Resolved Fluorescence Anisotropy Studies

The molecular dimensions of dendrimers have been previously estimated using intrinsic viscosity measurements<sup>36</sup> or by diffusion-ordered nuclear magnetic resonance.<sup>37</sup> However, these techniques generally require relatively high dendrimer concentrations and, therefore, must be performed in good solvents. To measure the secondary structural propensities of the dendrimers by circular dichroism as a function of hydrodynamic volume, a property greatly affected by solvent quality,<sup>38</sup> it was essential

to determine the molecular dimensions of the dendrimers in solvents of varying quality at micromolar concentrations that minimized aggregation and were comparable to the concentrations required for the circular dichroism measurements. The high sensitivity of fluorescence measurements ideally suited time-resolved fluorescence anisotropy (TRFA)<sup>39</sup> as a method to estimate the degree of compaction imparted to the dendrimer structure as a function of solvent, the nature of the connector, and dendrimer generation at low concentrations. Accordingly, the hydrodynamic properties of the dendrimers were measured by TRFA measurements<sup>40</sup> using the time-correlated single-photon counting (TCSPC) method<sup>41</sup> as a function of the dendrimer series, generation level, and solvent. Fluorescence anisotropy decays showed a biexponential profile consisting of a fast (10–30 ps) and a slow depolarization component (190–2000 ps). The fast decay component likely represents an intramolecular energy transfer depolarization process,<sup>38</sup> consistent with the presence of a delocalized excited state, whereas the slow component corresponds to the global rotation of the molecule. The hydrodynamic volumes ( $V_h$ ) were calculated from these values of the rotational correlation times ( $\Theta_2$ ) via the

(32) Demas, J. N. *Excited-State Lifetime Measurements*; Academic Press: New York, 1983.

(33) (a) Maus, M.; Mitra, S.; Lor, M.; Hofkens, J.; Weil, T.; Herrmann, A.; Muellen, K.; De Schryver, F. C. *J. Phys. Chem. A* **2001**, *105*, 3961. (b) Maus, M.; De, R.; Lor, M.; Weil, T.; Mitra, S.; Wiesler, U.-M.; Herrmann, A.; Hofkens, J.; Vosch, T.; Muellen, K.; De Schryver, F. C. *J. Am. Chem. Soc.* **2001**, *123*, 7668. (c) Schweitzer, G.; Gronheid, R.; Jordens, S.; Lor, M.; De Belder, G.; Weil, T.; Reuther, E.; Muellen, K.; De Schryver, F. C. *J. Phys. Chem. A* **2003**, *107*, 3199.

(34) (a) Shortreed, M. R.; Swallen, S. F.; Shi, Z.-Y.; Tan, W.; Xu, Z.; Devadoss, C.; Moore, J. S.; Kopelman, R. *J. Phys. Chem. B* **1997**, *101*, 6318. (b) Swallen, S. F.; Kopelman, R.; Moore, J. S.; Devadoss, C. *J. Mol. Struct.* **1999**, *485–486*, 585. (c) Swallen, S. F.; Shi, Z.-Y.; Tan, W.; Xu, Z.; Moore, J. S.; Kopelman, R. *J. Lumin.* **1998**, *76–77*, 193. (d) Swallen, S. F.; Zhu, Z.; Moore, J. S.; Kopelman, R. *J. Phys. Chem. B* **2000**, *104*, 3988.

(35) Olmsted, J. *J. Phys. Chem.* **1979**, *83*, 2581.

(36) Mourey, T. H.; Turner, S. R.; Rubinstein, M.; Frechet, J. M. J.; Hawker, C. J.; Wooley, K. L. *Macromolecules* **1992**, *25*, 2401.

(37) Young, J. K.; Baker, G. R.; Newkome, G. R.; Morris, K. F.; Johnson, C. S. *J. Macromolecules* **1994**, *27*, 3464.

(38) (a) De Backer, S.; Prinzie, Y.; Verheijen, W.; Smet, M.; Desmedt, K.; Dehaen, W.; De Schryver, F. C. *J. Phys. Chem. A* **1998**, *102*, 5451. (b) Hofkens, J.; Latterini, L.; De Belder, G.; Gensch, T.; Maus, M.; Vosch, T.; Karni, Y.; Schweitzer, G.; De Schryver, F. C.; Herrmann, A.; Mullen, K. *Chem. Phys. Lett.* **1999**, *304*, 1. (c) Tande, B. M.; Wagner, N. J.; Mackay, M. E.; Hawker, C. J.; Jeong, M. *Macromolecules* **2001**, *34*, 8580.

(39) For examples of time-resolved fluorescence depolarization studies on dendrimers, see refs 38a,b and: Matos, M. S.; Hofkens, J.; Verheijen, W.; De Schryver, F. C.; Hecht, S.; Pollak, K. W.; Frechet, J. M. J.; Forier, B.; Dehaen, W. *Macromolecules* **2000**, *33*, 2967.

(40) Fleming, G. R. *Chemical Applications of Ultrafast Spectroscopy*; Oxford University Press: New York, 1986.

(41) Buterbaugh, J. S.; Toscano, J. P.; Weaver, W. L.; Gord, J. R.; Hadad, C. M.; Gustafson, T. L.; Platz, M. S. *J. Am. Chem. Soc.* **1997**, *119*, 3580.

Debye–Stokes–Einstein relation (DSE):

$$\Theta = \frac{V_h \eta C f}{kT}$$

where  $\eta$  is the viscosity of the solvent,  $k$  is the Boltzmann constant, and  $T$  is the absolute temperature. The shape factor  $f$  corrects for the shape of the rotating molecule if the molecule is not spherical ( $f = 1$  for spherical molecules).<sup>40</sup>  $C$  is a measure of the coupling of the rotating solute and solvent molecules and has a value of 1 when the solute is much larger than the solvent.<sup>42</sup> Because the lowest molecular weight dendrons in this study are at least 10–100 times larger than the volume of the solvent and the rotating rotors are approximately spherical, a value of 1 is used for  $f$  and  $C$  (see Table 1 in Supporting Information for rotational correlation times ( $\phi$ ), hydrodynamic volume ( $V_h$ ), and free volume ( $V_{\text{free}}$ ) for dendrons and dendrimers as a function of solvent).

Comparing the measured hydrodynamic volume ( $V_h$ ) to the calculated van der Waals volume ( $V_{\text{vw}}$ ), calculated from Edwards increments<sup>43</sup> ( $V_h/V_{\text{vw}}$ ), provides an estimate of the packing efficiency wherein a lower ratio indicates tighter packing (proteins typically have  $V_h/V_{\text{vw}}$  ratios of 1.2–1.4<sup>44</sup>). Inspection of the  $V_h/V_{\text{vw}}$  ratios listed in Table 1 (Supporting Information) and Figure 6 revealed several noteworthy trends: (1) All ortho-linked dendrimers exhibited significantly higher packing efficiencies (lower  $V_h/V_{\text{vw}}$ ), ranging from 0.81 to 1.68, than their para-linked counterparts, which maintained  $V_h/V_{\text{vw}}$  ratios ranging from 1.55 to 6.3. (2) The hydrodynamic volumes of the para-linked dendrimers displayed higher solvent sensitivity than those of the corresponding ortho-linked dendrimers. This increased solvent sensitivity evolved from the relatively expanded conformations of the para-linked dendrimer, which support greater free volumes ( $V_h - V_{\text{vw}}$ ) that collapse in poor solvents. (3) In both series, going from the first to second generation resulted in a more tightly packed conformation. (4) Generally, solvents expanded the dendrimer structures in the order THF > CH<sub>2</sub>Cl<sub>2</sub>  $\approx$  MeCN. Interestingly, whereas the addition of 50% ethanol to CH<sub>2</sub>Cl<sub>2</sub> or MeCN dramatically collapsed the structures, the addition of 10% ethanol to CH<sub>2</sub>Cl<sub>2</sub> expanded the dendrimer structures.

### Conformational Studies

The TRFA studies established that linking the dendrons to the central core through a 2-aminobenzamide (ortho-linked) produces a more efficiently packed structure than linking through a 4-aminobenzamide (para-linked). Accordingly, circular dichroism studies could be used to establish the effect of the differential compaction levels, under a specific set of solvent and temperature conditions, on the degree and stability of chiral secondary structure expressed by the dendrons linked through the central core. During previous conformational studies on dendrons **1a–3**,<sup>25b,d</sup> we found that the transition that occurs in the CD spectra in the region of 300–340 nm is exclusively due to a  $\pi \rightarrow \pi^*$  transition of the anthranilamide chromophores. Time-dependent density functional calculations determined that this transition, centered at 316 nm, is polarized along the axis

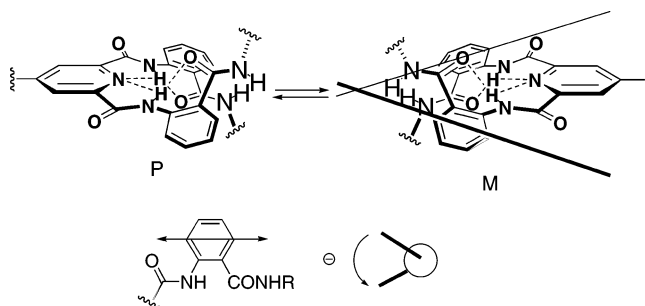


Figure 7. Helical interconversion of anthranilamide chromophores.

containing C3 and C6 as shown in Figure 7. Further, using the direction of the electric transition dipole moment, the excitonic couplet occurring at 316 nm in the CD spectra could be correlated with the helical relationship (M or P) between two adjacent anthranilamide chromophores (Figure 7). Thus, the bias of the dynamic equilibrium interconverting two diastereomeric helical conformations (M and P helices) relating a pair of anthranilamide termini could be determined.

### First-Generation Dendrimers

Comparison of the volumes determined by TRFA of *o*-link-[G1]-dend **7c** and *p*-link-[G1]-dend **8c** revealed three characteristic trends (Table 1 (Supporting Information), Figure 6). (1) *o*-Link-[G1]-dend **7c** maintained a significantly more compact global structure than did *p*-link-[G1]-dend **8c** in all solvents (e.g.,  $V_h/V_{\text{vw}}(\text{MeCN}) = 1.68$  (**7c**); 4.86 (**8c**)). (2) The hydrodynamic volume ( $V_h$ ) of *o*-link-[G1]-dend **7c** exhibited very little solvent sensitivity relative to that of *p*-link-[G1]-dend **8c**, indicating the presence of a highly compact structure not having significant free volume ( $V_{\text{free}}$ ). (3) In contrast, *p*-link-[G1]-dend **8c** exhibited a maximum  $V_h$  in THF, a minimum  $V_h$  in 50% ethanol/MeCN, and expanded slightly upon the addition of 10% ethanol to a CH<sub>2</sub>Cl<sub>2</sub> solution of the dendrimer. Interestingly, although dendrons **7b** and **8b** exhibited simple Cotton effects at 316 nm, indicating an unbiased helical equilibrium, dendrimers **7c** and **8c** exhibited strong, negative excitonic couplets centered at 316 nm in MeCN at  $-20$  °C (Figure 8). The negative chirality of the couplet is consistent with a shift in the conformational equilibrium toward the M helical conformation. This excitonic couplet was relatively insensitive to temperature up to 60 °C in THF and MeCN for **7c**, whereas the couplet for **8c** was highly sensitive to increasing temperature in MeCN and the couplet was extremely weak at any temperature in THF. This chiroptical behavior correlates well with the packing efficiency displayed by the dendrimers. For example, the  $V_h/V_{\text{vw}}$  ratio was similarly low for **7c** in THF and MeCN, indicating that the packing efficiency was an intrinsic property of the ortho-linked dendrimer structure and relatively insensitive to solvent quality. In contrast, **8c** exhibited an expanded conformation in MeCN ( $V_h/V_{\text{vw}} = 4.86$ ) that expanded further in THF ( $V_h/V_{\text{vw}} = 6.3$ ). Accordingly, the conformational behavior of **7c** was similarly temperature-insensitive in THF and MeCN, whereas **8c** did not show a helical bias in THF and exhibited a highly temperature-dependent helical bias in MeCN. The correlation of low values of  $V_h/V_{\text{vw}}$  with an increase in the level and stability of chiral secondary structure suggests that compacting the dendrimer structure is an important factor in reinforcing the secondary structural propensity of the dendrimers.

(42) Hartman, R. S.; Konitsky, W. M.; Waldeck, D. H.; Chang, Y. J.; Castner, E. W. *J. Chem. Phys.* **1997**, *106*, 7920.

(43) Edward, J. T. *J. Chem. Educ.* **1970**, *47*, 261.

(44) Chalikian, T. V.; Totrov, M.; Abagyan, R.; Breslauer, K. J. *J. Mol. Biol.* **1996**, *260*, 588.

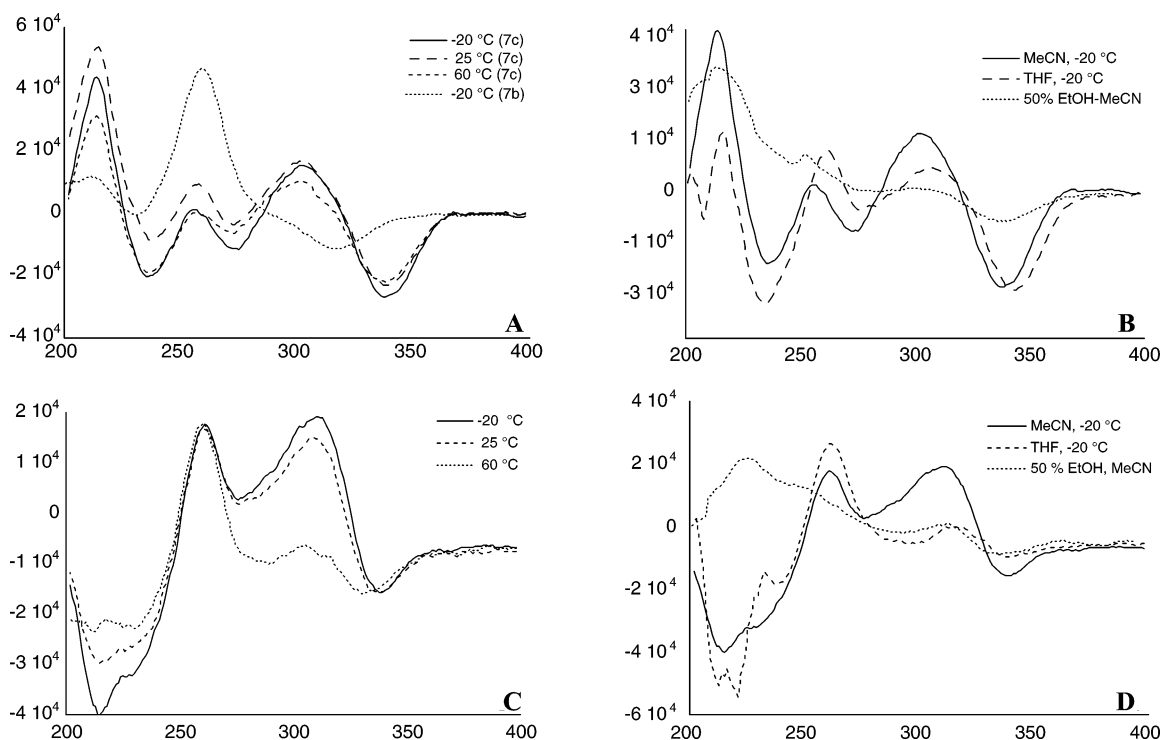


**Figure 8.** Circular dichroism spectra (normalized for concentration and number of terminal groups) of first-generation dendron and dendrimers as a function of solvent, temperature, and linkage: (A) *o*-link-[G1]-dend **7c** and dendron **7b** in MeCN as function of temperature. (B) *o*-link-[G1]-dend **7c** as a function of solvent at  $-20$  °C. (C) *p*-link[G1]-dend **8c** as a function of temperature. (D) *p*-link[G1]-dend **8c** as a function of solvent at  $-20$  °C.

The addition of 50% ethanol (a poor dendrimer solvent) to MeCN resulted in the most compact structures for both **7c** ( $V_h/V_{vw} = 1.17$ ) and **8c** ( $V_h/V_{vw} = 1.73$ ). Unexpectedly, in this solvent system, neither dendrimer exhibited a significant helical bias. We have previously observed that the addition of 10% ethanol reduces or destroys the helical bias of chiral dendrons.<sup>25b</sup> This observation was attributed to the partial disruption of the intramolecular hydrogen-bonding interactions in the presence of small amounts of ethanol. Therefore, it is noteworthy that both **7c** and **8c** slightly expand when 10% ethanol is added to  $\text{CH}_2\text{Cl}_2$  solutions of the dendrimers whereas at 50% ethanol, a dramatic structural collapse occurs. Consequently, this behavior can be attributed to a partial disruption of the intramolecular hydrogen-bonding interactions at low concentrations of ethanol that reduces the conformational order in a manner that slightly increases the hydrodynamic volume of the dendrimers. Because ethanol is a poor solvent for the dendrimers (i.e., the dendrimers are insoluble in pure ethanol), at higher concentrations the partially denatured structure experiences a nonspecific collapse resulting in a compact structure lacking a helical bias. Therefore, we conclude, in this case, that an increase in secondary structural order will occur only when the dendrimer collapses in a manner that results in specific nonlocal interactions between elements of local secondary structure in contrast to a nonspecific structural collapse.

### Second-Generation Dendrimers

We previously reported that the second-generation dendron **2a** exhibited a highly thermally stable (up to  $110$  °C) and solvent-insensitive helical conformational order as evidenced by circular dichroism and NOESY NMR spectroscopy.<sup>25d</sup> This unusual thermal stability was attributed to the synchronization of internal and peripheral conformational equilibria within the

dendron and to the greater overall packing efficiency of the folded state. The highly compact structure of **2a** was confirmed by TRFA studies that revealed  $V_h/V_{vw}$  ratios ranging from 1.06 in MeCN to 2.0 in THF. Moreover, *o*-link-[G2]-dend **9c** maintained an even more compact morphology than **2a** in all of the solvents studied. Accordingly, CD studies for *o*-link-[G2]-dend **9c** indicated a greater bias for the M helical conformation, relative to dendron **2a**, as evidenced by the increased magnitude of the excitonic couplet centered at 316 nm. Surprisingly, the CD spectra of **9c**, in contrast to the isolated dendron **2a**, were extremely solvent and temperature dependent (Figure 9). For example, the couplet was present in MeCN; however, in THF or 50% ethanol/ $\text{CH}_2\text{Cl}_2$ , a significantly decreased couplet intensity was observed. These solvent effects correlate well with the associated solvent-induced changes in the  $V_h/V_{vw}$  ratios for THF and MeCN. For example, *o*-link-[G2]-dend **9c** exhibited a larger volume in THF ( $V_h/V_{vw} = 1.5$ ) than in MeCN ( $V_h/V_{vw} = 0.94$ ). However, similar to *p*-link-[G1]-dend **8c**, **9c** expanded slightly upon the addition of 10% ethanol to  $\text{CH}_2\text{Cl}_2$  and dramatically collapsed in 50% ethanol/ $\text{CH}_2\text{Cl}_2$ , exhibiting no helical bias in the compact state. Additionally, heating the sample to  $60$  °C in MeCN resulted in a lack of any helical bias, in contrast to the thermally stable bias present in dendron **2a**. Similar to the first-generation dendrimers (**7c** and **8c**), *o*-link-[G2]-dend **9c** exhibited significantly lower  $V_h/V_{vw}$  ratios than the isomeric para-linked dendrimer (*p*-link-[G2]-dend, **10c**). The hydrodynamic volumes of both dendrimers exhibited a similar solvent sensitivity profile (Figure 6). This behavior is in qualitative agreement with dendrimers **7c** and **8c**; however, *o*-link-[G2]-dend **9c** and *p*-link-[G2]-dend **10c** were more compact than their first-generation counterparts, **7c** and **8c**, and exhibited qualitatively similar, but greater overall, sensitivity to solvent. *p*-Link-[G2]-dend **10c** also exhibited a

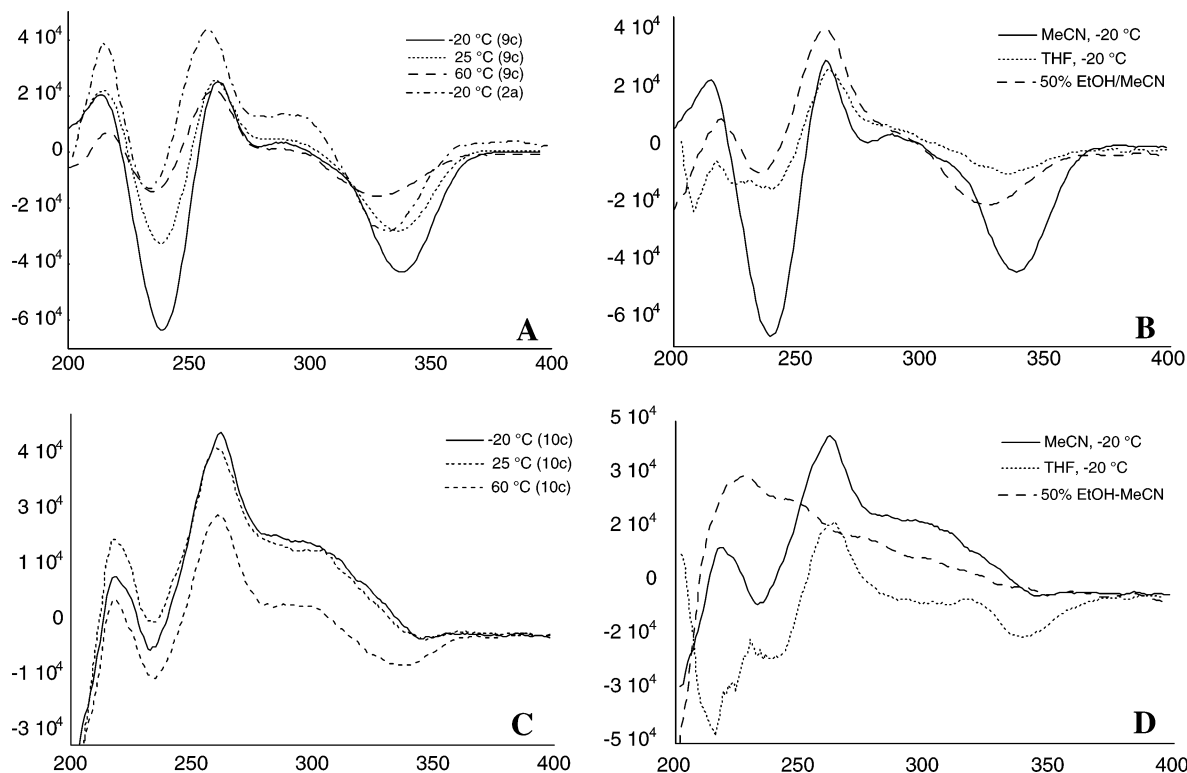


**Figure 9.** Circular dichroism spectra (normalized for concentration and number of terminal groups) of second-generation dendron and dendrimers as a function of solvent, temperature, and linkage: (A) *o*-link-[G2]-dend **9c** and dendron **2a** in MeCN as function of temperature. (B) *o*-link-[G2]-dend **9c** as a function of solvent at  $-20\text{ }^{\circ}\text{C}$ . (C) *p*-link-[G2]-dend **10c** as a function of temperature. (D) *p*-link-[G2]-dend **10c** as a function of solvent at  $-20\text{ }^{\circ}\text{C}$ .

couplet in the CD spectra that was maximal in MeCN and minimal in THF, similar to *o*-link-[G2]-dend **9c**; however, the intensity was greatly reduced relative to **9c**.

### Third-Generation Dendrimers

Unfortunately, at the third generation, determination of the hydrodynamic volumes was not possible because the fluorescence depolarization curve was dominated by the fast component of the process, which became increasingly dominant going from the first- to the third-generation dendrimers. Nevertheless, it is likely that the trend of increasing compactness going from the first to second generation continues upon progressing to the third-generation dendrimers. Surprisingly, in MeCN, the CD spectra of the *o*-link-[G3]-dend, **11c**, exhibited a positive excitonic couplet, indicating that a shift in equilibrium toward the P helical conformation occurred, in contrast to the M-helical bias present in all of the other dendrons and dendrimers (Figure 10). Interestingly, increasing the temperature or changing solvent to THF or 50% ethanol/MeCN reverts the couplet to negative chirality, indicating a return to an M helical bias, similar in magnitude to the third-generation dendron **3**. Although this unique conformational preference cannot be fully rationalized, it is consistent with the general trend observed beginning at the second generation for the nonlocal interactions to oppose the secondary structural preference of the isolated dendrons. In contrast, *p*-link-[G3]-dend **12c** exhibits an M helical bias only slightly lower in magnitude to dendron **3**. Changing solvent to THF or 50% EtOH/MeCN decreases the amplitude of the couplet similar to the effect of these solvents on the first- and second-generation dendrimers of both series.

### Discussion

The degree of structural compaction correlates closely with the extent and stability of secondary structural bias when comparing the ortho-linked dendrimers (**7c**, **9c**, **11c**), having highly compact structures, to the para-linked counterparts (**8c**, **10c**, **12c**) exhibiting relatively expanded conformations. This correlation is most apparent for the first-generation dendrimers *o*-link-[G1]-dend **7c** and *p*-link-[G1]-dend **8c**. For example, although the parent dendron, **1a**, exhibits no helical bias, assembling the dendrons into *o*-link-[G1]-dend **7c** produces a highly compact structure with a strong M helical bias that is thermally stable and insensitive to solvent quality. In contrast, the expanded structure of para-linked isomer **8c** displays a relatively unstable secondary structure. Moreover, the helical bias is lost going from MeCN to the more expanded conformation in THF. This correlation also holds when comparing the *o*-link-[G2]-dend **9c** and *p*-link-[G2]-dend **10c**. Accordingly, *o*-link-[G2]-dend **9c**, which is significantly more compact than *p*-link-[G2]-dend **10c**, exhibits far greater secondary structure than **10c**, and both **9c** and **10c** lose secondary order in THF, which expands the dendrimers relative to MeCN. However, there are several observations that do not directly correlate the secondary order with the extent of dendrimer compaction. For example, although the dendrimers collapse to their most compact forms in 50% ethanol/MeCN, a minimal helical bias is observed for all dendrimers in this solvent system. Similarly, with the exception of the first-generation dendrimers, **7c** and **8c**, the dendrons exhibit a greater and more stable secondary structural bias than the corresponding dendrimers, which are uniformly more compact than the associated dendrons. Thus, second-generation dendron **2a** maintains a high helical bias even at 110

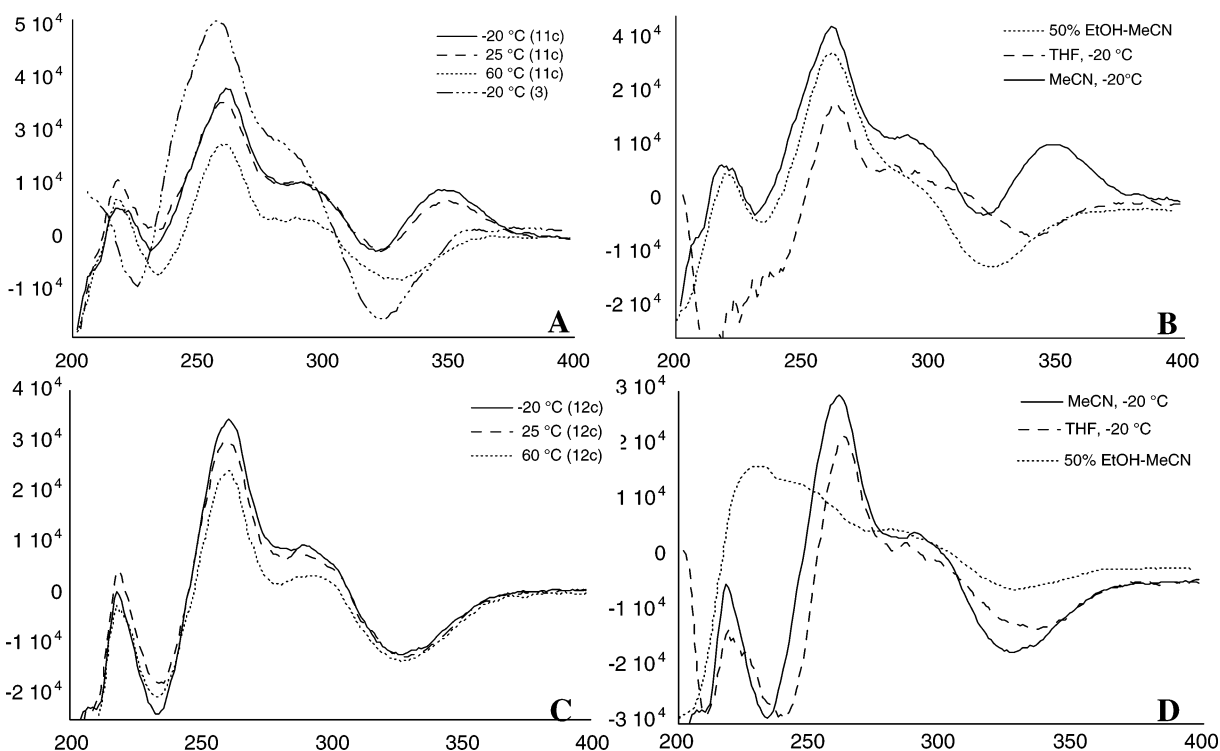


**Figure 10.** Circular dichroism spectra (normalized for concentration and number of terminal groups) of second-generation dendron and dendrimers as a function of solvent, temperature, and linkage: (A) *o*-link-[G3]-dend **11c** and dendron **3** in MeCN as function of temperature. (B) *o*-link-[G3]-dend **11c** as a function of solvent at  $-20\text{ }^{\circ}\text{C}$ . (C) *p*-link[G3]-dend **12c** as a function of temperature. (D) *p*-link[G3]-dend **12c** as a function of solvent at  $-20\text{ }^{\circ}\text{C}$ .

$^{\circ}\text{C}$ , whereas the corresponding dendrimer **9c** experiences a complete loss of bias at  $60\text{ }^{\circ}\text{C}$  and the para-linked isomer **10c** shows little bias at all temperatures. Finally, in contrast to the M helical preference of all of the other dendrons and dendrimers, ortho-linked third-generation dendrimer **11c** switches to a P helical preference in MeCN at low temperature, reverting to an M bias at higher temperatures or in a structure-expanding solvent such as THF. These apparent anomalies indicate that, although compaction can enhance secondary structural propensities, the nature of compaction is more important than the extent of compaction in determining the amount and stability of local secondary structure. Specifically, these anomalies suggest that local secondary structure in the dendrimers is enhanced when compaction packs the subunits in a mutually complementary fashion that synchronizes conformational equilibria. Alternatively, the nonspecific collapse of a structure may induce a perturbation of local secondary order in a manner that maximizes packing but opposes the intrinsic local order, resulting in a decrease or a change in helical bias. For example, the loss of secondary structure upon the addition of ethanol to the solvent can be understood by the observation that adding a small amount (10%) expands the structures. The protic nature of ethanol partially disrupts the intramolecular interactions that stabilize the local helical conformation, leading to a disordering of the local helical conformation and an expansion of the structure, whereas at higher concentrations (50%), ethanol behaves as a poor dendrimer solvent, inducing a nonspecific collapse of this disordered structure. Similarly, model-building studies suggest that the 2-aminobenzamide linkage present in *o*-link-[G1]-dend **7c** arranges the dendrons around the central core in a propeller-like arrangement that packs mutually complementary faces of the dendrons together. This complementary packing synchronizes conformational equilibria in the dendrons in a manner that

amplifies the small M helical bias of the parent dendron. Linking these dendrons through a 4-aminobenzamide function orients the dendrons in a radially expanded conformation, causing the dendrons to potentially interact via several different orientations. This decreases the complementarity and efficiency of packing, resulting in a lowered helical bias. Why is the helical bias less pronounced at higher generations even though compaction has increased? We hypothesize that the nonspecific, intramolecular interactions between adjacent dendrons increase at higher generations as a consequence of the steric congestion that normally develops among the branches and at the surface of dendrimers. In *o*-link-[G2]-dend **9c**, these nonspecific interactions compete with the tendency of the 2-aminobenzamide linkage to pack the dendrons in a complementary fashion, resulting in a thermally unstable helical bias, relative to dendron **2a**. The 4-aminobenzamide linkage reduces the packing complementarity further so that the nonspecific interactions dominate, leading to a loss of secondary order. These nonspecific effects are enhanced at *o*-link-[G3]-dend **11c** to the extent that a shift in the local helical equilibria toward a P helical bias occurs. Decreasing the nonspecific packing with the 4-aminobenzamide linkage shifts the equilibria back to an M bias, albeit slightly lower in extent than parent dendron **3**. It is noteworthy that a shift from a P to M bias also occurs in *o*-link-[G3]-dend **11c** upon going from MeCN to THF, which expands the structures of all of the other dendrimers, and is consistent with the hypothesis that nonspecific packing of the dendrimer structure is responsible for the shift to a P helical bias.

## Conclusion

In contrast to dendrimers constructed from flexible subunits, relatively minor modifications in the structure of folded dendrimers, composed of dendrons exhibiting rigid, folded con-

formations, afford large variations in hydrodynamic volumes. Further, the concomitant changes in overall compaction greatly affect the intrinsic local secondary structural preferences of the constituent dendrons. It is noteworthy that the most rapidly folding biopolymers in nature exhibit a near perfect balance between local and nonlocal interactions, producing intermediates along the folding pathway that maintain an overall topology similar to that of the native state to minimize the creation of nonnative interactions that inhibit the folding process.<sup>45</sup> Similar to protein folding, dendrimer compaction must occur in a manner that preserves the topology of the folded dendron structure. A reinforcement of the local conformational preferences of the dendrons occurs when compaction packs the dendrons in a mutually complementary fashion. Packing mutually complementary surfaces together reinforces secondary structural preferences, resulting in greater or more stable

(45) Millet, I. S.; Townsley, L. E.; Chiti, F.; Doniach, S.; Plaxco, K. W. *Biochemistry* **2002**, *41*, 321.

secondary structure with increasing compaction. In contrast, nonspecific compaction increases the nonlocal interactions between adjacent dendrons but not necessarily in a manner that preserves the dendron topology and may oppose local secondary preferences.

**Acknowledgment.** This work was supported by the National Science Foundation (CHE-0239871).

**Supporting Information Available:** Experimental procedures, complete analytical data for compounds **1–12**, lifetime data for **3** and **7c**, a table of rotational correlation times ( $\phi$ ), hydrodynamic volumes ( $V_h$ ) and free volume ( $V_{free}$ ) for dendrons and dendrimers as a function of solvent; experimental setup details for TCSPC and fluorescence studies; and copies of the <sup>1</sup>H NMR and mass spectral data for dendrimers **7c–12c** (PDF). This material is available free of charge via the Internet at <http://pubs.acs.org>.

JA037895A